Pergamon

www.elsevier.com/locate/neuroscience

PII: S0306-4522(00)00173-1

Neuroscience Vol. 99, No. 2, pp. 333–342, 2000

0306-4522/00 $20.00+0.00

FUNCTIONAL ROLE AND THERAPEUTIC IMPLICATIONS OF NEURONAL CASPASE-1 AND -3 IN A MOUSE MODEL OF TRAUMATIC SPINAL CORD INJURY

M. LI,* V. O. ONA,* M. CHEN,* M. KAUL,†‡ L. TENNETI,†‡ X. ZHANG,§ P. E. STIEG,* S. A. LIPTON†‡ and R. M. FRIEDLANDER* ‖

*Neuroapoptosis Laboratory and Neurosurgical Service, Department of Surgery, †Cerebrovascular and Neuroscience Research Institute, and §Cardiovascular Division, Department of Medicine, Brigham and Women's Hospital, Harvard Medical School, Boston, MA 02115, USA

Abstract—Evidence indicates that both necrotic and apoptotic cell death contribute to tissue injury and neurological dysfunction following spinal cord injury. Caspases have been implicated as important mediators of apoptosis following acute central nervous system insults. We investigated whether caspase-1 and caspase-3 are involved in spinal cord injury-mediated cell death, and whether caspase inhibition may reduce tissue damage and improve outcome following spinal cord injury. We demonstrate a 17-fold increase in caspase-1 activity in traumatized spinal cord samples when compared with samples from sham-operated mice. Caspase-1 and caspase-3 activation were also detected by western blot following spinal cord injury, which was significantly inhibited by the broad caspase inhibitor *N*-benzyloxycarbonyl-Val-Ala-Asp-fluoromethylketone. By immunofluorescence or *in situ* fluorogenic substrate assay, caspase-1 and caspase-3 expression were detected in neuronal and non-neuronal cells following spinal cord injury. *N*-Benzyloxycarbonyl-Val-Ala-Asp-fluoromethylketone treated mice, and transgenic mice expressing a caspase-1 dominant negative mutant, demonstrated a significant improvement of motor function and a reduction of lesion size compared with vehicle-treated mice.

Our results demonstrate for the first time that both caspase-1 and caspase-3 are activated in neurons following spinal cord injury, and that caspase inhibition reduces post-traumatic lesion size and improves motor performance. Caspase inhibitors may be one of the agents to be used for the treatment of spinal cord injury. © 2000 IBRO. Published by Elsevier Science Ltd. All rights reserved.

Key words: apoptosis, ICE, zVAD-fmk, interleukin-1β, neuroprotection.

In the United States, there are 183,000–230,000 people surviving with disabilities resulting from spinal cord injury (SCI) with approximately 10,000 new cases occurring each year.[1] More than half of SCI survivors cannot return to their normal life.[2] This disappointing prognosis results in part due to the poor understanding of the mechanism mediating secondary degeneration. Neurological damage after acute SCI results from both the primary mechanical injury as well as the subsequent activation of cell death cascades mediating delayed tissue damage.[3] The primary injury results from actual mechanical tissue disruption, as well as necrotic cell death. Secondary degeneration results from a cascade of events triggered by the injury, resulting in activation of endogenous cell death pathways.[4,5] High dose steroids, the widely used treatment for SCI, target many mediators of secondary degeneration, but outcome remains disappointing.[6] Reports have identified apoptosis or programmed cell death as an important component contributing to tissue damage following SCI in rats, monkeys, as well as humans.[4,5,7–10] Apoptotic cell death has been detected up to three weeks following SCI.[8] Since apoptosis is a tightly regulated process, this finding provides the opportunity to manipulate apoptotic pathways for the treatment of SCI.

The critical role of the caspases in apoptosis is well known.[11,12] Caspase-1 [interleukin-1β converting enzyme, (ICE)] has been implicated as a critical mediator of apoptosis following both acute CNS insults (ischemia and trauma) as well as models of chronic neurodegeneration (amyotrophic lateral sclerosis, Parkinson's disease and Huntington's disease).[13,19] In these animal models, caspase-1 activation has been demonstrated, and caspase inhibition not only reduced tissue damage, but also resulted in improved neurological function.[13,15] Caspase-3 activation has also been demonstrated in ischemia and trauma as well as in humans following SCI.[9,10,20,21] Significant insight regarding *in vivo* neuronal cell death has been generated using a transgenic mouse expressing a caspase-1-dominant negative mutant.[14,16–18] The transgene is caspase-1 with its active site cysteine (C285) substituted for a glycine (M17Z). The caspase-1 mutant is an effective caspase-1-dominant negative inhibitor (and possibly of other caspase family members). The neuron-specific enolase promoter targets transgene expression to neurons, oligodendrocytes, and astrocytes (NSE-M17Z).[14,22,23] Using this mouse, as well as a pharmacologic approach to inhibit caspases, we investigated whether caspase-1 and caspase-3 are activated following SCI, and if their inhibition would reduce post-traumatic lesion size and improve neurological recovery.

EXPERIMENTAL PROCEDURES

Spinal cord injury model

A total of 110 mice (20–25 g) of the C57BL/6 strain (Jackson Lab,

‡Present address: The Burnham Institute, 10901 North Torrey Pines Road La Jolla, CA 92037, USA.

‖To whom correspondence should be addressed. Tel.: +1-617-732-7676; fax: +1-617-734-8342.

E-mail address: rfriedlander@rics.bwh.harvard.edu (R. M. Friedlander).

Abbreviations: ANOVA, analysis of variance; DEVD-CHO, *N*-acetyl-Asp-Glu-Val-Asp-CHO; DMSO, dimethylsulfoxide; EDTA, ethylenediaminetetra-acetate; ELISA, enzyme-linked immunosorbent assay; HRP, horseradish peroxide; ICE, interleukin-1β converting enzyme; IL-1β, interleukin-1β; NeuN, neuronal nuclei; NSE, neuron specific enolase; PBS, phosphate-buffered saline; PMSF, phenylmethylsulfonyl fluoride; SCI, spinal cord injury; SDS–PAGE, sodium dodecylsulfate–polyacrylamide gel electrophoresis; TE, tris ethylenediaminetetra-acetic acid; TUNEL, TdT-mediated dUTP nick-end labeling; zVAD-fmk, *N*-benzyloxycarbonyl-Val-Ala-Asp-fluoromethylketone.

Bar Harbor, ME, USA), or NSE-M17Z mice and wild-type littermates, which we generated in a C57BL/6 background, were used in this study. Transgenic mice were genotyped as previously described.[14] All efforts were made to minimize both suffering and number of animals used. All experimental procedures were in accordance with protocols approved by the Harvard Medical School Animal Care Committee. Mice were anesthetized with an i.p. injection of 2,2,2-tribromoethanol (0.02 ml of a 2.5% solution/g body weight). After the depth of anesthesia was adequate, the mouse was placed prone in a modified spinal stereotactic apparatus with vertebral column fixation under a stereomicroscope. The skin was shaved and decontaminated. A 15–20-mm midline incision was made, and the T7–T12 levels were exposed by laterally separating the dorsal para-spinous muscles. Trauma was performed using a modification of the weight-drop method.[24] Briefly, a T8, T9, and T10 laminectomy was made with a high-speed micro drill (Harvard apparatus, Inc. Holliston, MA, USA) and a micro-rongeur (Fine Science Tools, Inc. Foster City, CA, USA) Following the laminectomy, a window over the dura of at least 1.6 mm in diameter was made to accommodate a stainless steel impact rod with a diameter of 1.4 mm and weight of 1.8 g. Part of the dura mater was carefully removed though the window for better drug penetration. Two horizontal bars of the stereotactic frame were used for vertebral column stabilization by clamping the T9–T10 transverse processes bilaterally. A vertical bar of the stereotactic frame held the cylinder supporting the weight rod, which was raised 10 mm above the dura and dropped onto the spinal cord at the T9 level. Following trauma, mice were randomly divided into two groups and treated with *N*-benzyloxycarbonyl-Val-Ala-Asp-fluoromethylketone (zVAD-fmk) or vehicle [dimethylsulfoxide (DMSO) 0.4%] (Enzyme Systems, Livermore, CA, USA). A piece of surgical gelfoam ($2\times2\times6$ mm^3) presoaked in 10 μl of zVAD-fmk (10 μg) or vehicle was placed over the contused spinal cord. The muscle and skin were sutured in layers. During surgery, mice were kept on a 37°C warming blanket, and after surgery recovered in a 37°C incubator until fully alert. The bladder was manually expressed twice daily until return of reflexive bladder control. Animals had free access to food and water. The trauma model was equivalent in the NSE-M17Z and wild-type mice, with all the mice receiving vehicle treatment.

TdT-mediated dUTP nick-end labeling and immunohistochemistry

NSE-M17Z, zVAD-fmk or wild-type vehicle-treated mice were transcardiacly perfused with 4% paraformaldehyde (pH 7.4) in phosphate buffer 8, 24 and 48 h after trauma. Samples were embedded in paraffin, and cut in 10-μm sections. TdT-mediated dUTP nick-end labeling (TUNEL) assay was carried out using a Fluorescein Apoptosis Detection Kit (Promega, Madison, WI, USA) Hoechst 33342 (Molecular Probe, Eugene, OR, USA) was used to evaluate nuclear morphology. Neurons were identified using anti-neuronal nuclei (NeuN) antibody (Chemicon, Temecula, CA, USA)

Mature interleukin-1β determination

Mature interleukin-1β (IL-1β) concentration was measured using an enzyme-linked immunosorbent assay (ELISA) kit (R&D Minneapolis, MN, USA) which is specific for mature IL-1β. Spinal cord tissue 15 mm long, centered upon the impact area, was removed from mice treated with zVAD-fmk or vehicle for 24 h after SCI or from sham-operated mice on which only a laminectomy and dural opening were preformed without trauma ($n=3$). Tissue was processed as previously described.[14]

Western blot analysis

Spinal cord tissue was lysed in RIPA buffer (150 mM NaCl, 1% Nonidet P-40, 12 mM sodium deoxycolate, 0.1% sodium dodecylsulfate (SDS), 50 mM Tris–HCl, pH 7.2), supplemented with protease inhibitors (PMSF, leupeptin, pepstatin A, and aprotinin). Lysates were centrifuged and protein concentration was determined using a protein assay (Bio-Rad, Hercules, CA, USA). Samples were loaded (50 μg of protein/lane), electrophoresed on a 15% SDS–polyacrylamide gel electrophoresis (SDS–PAGE) gel, and blotted to an Immobilon-P transfer membrane (Millipore, Bedford, MA, USA). Blots were probed with a monoclonal antibody against the caspase-1 p20 subunit (generously provided by Dr. Junying Yuan), or with a polyclonal antibody against the p17 subunit of caspase-3 (generously provided by Anu Srinivasan, Idun, La Jolla, CA, USA) and visualized with horseradish peroxidase-conjugated secondary antibodies by ECL (Amersham).

DNA laddering

Spinal cord DNA was isolated according to published methods.[25] Briefly, sham-operated mice and mice receiving zVAD-fmk or vehicle were euthanized 24 h after trauma. The tissue was homogenized in lysis buffer (10 mM Tris–HCl, 100 mM EDTA, and 0.5% SDS) and incubated with proteinase K (100 μg/ml). DNA was extracted by phenol/chloroform/amyl alcohol (25:24:1), precipitated with 70% ethanol, and resuspended in TE buffer. The samples were digested with DNase-free RNase, and separated by electrophoresis on a 1.5% agarose gel.

Detection of conformationally active caspase-3-like and caspase-1 proteases

To demonstrate activation of caspase-3 in SCI-induced neuronal apoptosis, we used an affinity-labeling technique with biotinylated-*N*-acetyl-Asp-Glu-Val-Asp-CHO (DEVD-CHO) (BIOMOL Research Laboratories, Inc., Plymouth Meeting, PA, USA), as previously described with some modifications.[26,27] At indicated times, following deparaffinization and rehydration, sections were washed with phosphate-buffered saline (PBS) containing 0.05% Tween-20 and blocked in 10% normal goat serum for 1 h. Next, tissue was incubated with 50 μM biotinylated-DEVD-CHO for 48 h at 4°C. Following three washes with PBS, tissue was incubated with fluorescein avidin DCS (1:1000, Vector Laboratories, Burlingame, CA, USA) for 30 min. For double staining with anti-caspase-3 antibody, CM1 (Idun, La Jolla, CA, USA) and bioltinylated-DEVD-CHO, sections were incubated with primary antibody CM1 (1:6000) overnight after biotinylated-DEVD-CHO incubation and followed by a 1-h incubation with anti-rabbit TEXRED (1:200, Vector Laboratories, Burlingame, CA, USA). For co-staining with anti-NeuN and bioltinylated-DEVD-CHO, the sections were incubated with anti-NeuN antibody (Chemicon, Temecula, CA, USA) in dilution of 1:100 for 1 h and then probed with anti-mouse TEXRED (1:200, Vector Laboratories, CA, USA). Hoechst 33342 (0.2 μg/ml, Molecular Probe, Eugene, OR, USA) was used for counterstaining. DEVD-associated fluorescence was detected using epifluorescence microscopy. For controls, tissue not treated with biotinylated-DEVD-CHO did not display staining, indicating that the affinity-labeling technique specifically detects conformationally active caspase-3-like proteases. Furthermore, preincubation with unlabeled DEVD-CHO (300 μM) greatly reduced biotinylated-DEVD-associated cellular fluorescence. For caspase-1 protease detection, specimens were incubated with a monoclonal antibody against the caspase-1 p20 subunit (generously provided by Dr Junying Yuan) at 1:3 dilution and probed with biotinylated anti-rat immunoglobulin followed by incubation in 1:1000 fluorescein avidin DCS for 1 h. The primary antibody was eliminated in controls, which did not reveal a detectable signal.

Quantification of apoptotic cells following spinal cord injury

To quantitatively compare the extent of apoptosis following SCI in vehicle-treated, zVAD-fmk-treated, and caspase-1-dominant negative mice, we performed apoptotic cell counting on TUNEL-stained sections from each of these groups ($n=3$). The sections (10 μm thick) were obtained from the epicenter and 3 mm rostral and caudal to the impact site 24 h following SCI. A blinded researcher counted TUNEL-positive cells in five random high-power fields (40×) from each section using epifluorescence microscopy, without discriminating between white and gray matter.

Behavioral assessment

All animals were blindly scored on three different behavioral tests adopted from previously described methods for the evaluation of mouse SCI models,[24] including open field, pain withdrawal, and platform tests. Mice were evaluated on the day before surgery, on post-surgical days 3 and 7, and weekly thereafter for three weeks.

Lesion size measurement

On post-trauma day 28, animals were euthanized with isoflurane and transcardially perfused with heparinized saline followed by 4%

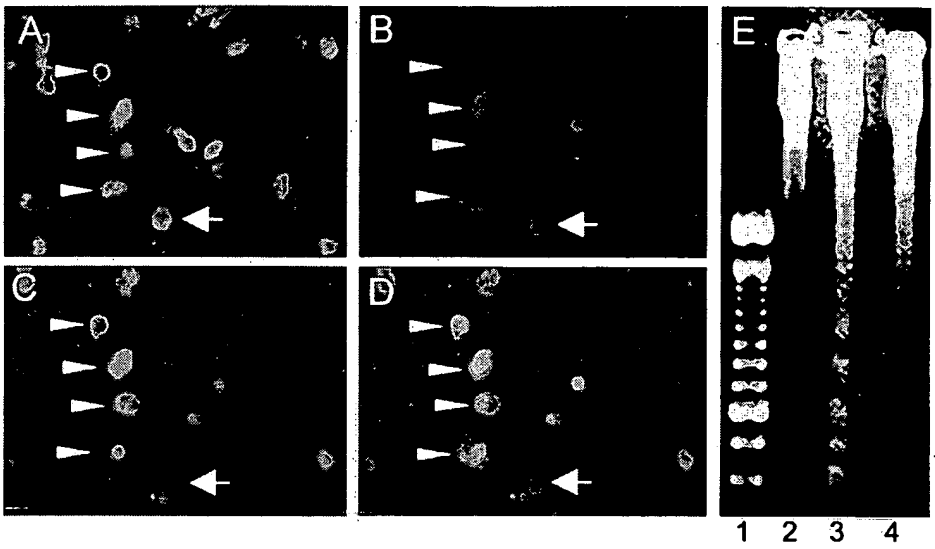

Fig. 1. Post-SCI neuronal apoptosis. (A–D) A traumatized spinal cord section at the lesion epicenter 24 h after SCI was stained with Hoechst 33342 (A), NeuN (B), and TUNEL (C); (D) is a superimposed image of (B) and (C). Yellow or orange cells in (D) (arrowheads) represent apoptotic neurons since they are TUNEL- and NeuN-positive. Green cells in (D) most likely represent non-neuronal apoptotic cells since they do not stain for NeuN. Non-apoptotic neurons in (D) are red (arrow). These results demonstrate that post-SCI apoptosis occurs in both neuronal and non-neuronal cells. (E) Ethidium bromide-stained agarose gel demonstrates a DNA ladder from a vehicle-treated mouse (lane 3) at 24 h after SCI. Laddering was virtually undetectable in traumatized zVAD-fmk-treated mice (lane 4) and was not visible in sham-operated mice (lane 2). Lane 1 shows 100-bp DNA ladder standard (this experiment was independently performed with three different sets of mice).

paraformaldehyde (pH 7.4) in PBS. Spinal cord segments 5 mm long (2.5 mm rostral and caudal to the impact site) were removed and post-fixed in paraformaldehyde overnight and then embedded in paraffin. Serial transverse sections (20 μm thick) were cut, and one of every 40 sections was saved for lesion size measurement. The sections were stained with Luxol Fast Blue, by which residual white and gray matter are easily distinguished from the lesioned area, and Cresyl Violet to visualize neurons.[24] The damaged area of spinal cord was characterized by neuronal loss and weakly stained tissue (Fig. 6B–E). The images of the stained specimen were captured by a digital photographic camera (Sony DKC-5000) and analysed with a Scion Image System (NIH image 6.1) for morphometric measurement. Total lesion volumes were computed by integrating the lesion area of each section and the distance between two sections (0.8 mm) (Total lesion volume = lesion area of section $1 \times 0.8/2$ + lesion area of section $2 \times 0.8/2$ + lesion area of section $3 \times 0.8/2 + \ldots +$ lesion area of section $10 \times 0.8/2$). All lesion volume analyses were performed by a blinded investigator.

Data analysis

Data are presented as mean ± S.E.M. Statistical comparisons among three different groups (vehicle-treated, zVAD-treated and NSE-M17Z) for lesion volumes were made by one-way analysis of variance (ANOVA) with post-test. The behavioral outcomes were analysed by a two-way ANOVA with repeated measures and significant two-way ANOVA was followed by the Scheffe test (acceptable $P < 0.05$) to perform a series of the mean comparisons. The statistical programs Statistical Analysis System and GraphPad InStar were used in the statistic analysis.

RESULTS

N-*Benzyloxycarbonyl-Val-Ala-Asp-fluoromethylketone treatment and caspase-1-dominant negative mutant expression inhibit post-spinal cord injury-mediated apoptosis*

To determine whether apoptotic cell death played a role in the mouse SCI weight drop model, we performed TUNEL staining and evaluated the presence of oligonucleosomal DNA degradation in traumatized spinal cord tissue. Apoptotic cells, some of which were stained with neuronal-specific markers, were incrementally detected at 8, 24 and 48 h following trauma (Figs 1A–D, 2A–C). Distinct oligonucleosomal DNA fragmentation was detected superimposed on random DNA degradation, represented as a smear of various molecular weights, suggesting that both apoptotic and necrotic cell death played a role in our mouse SCI model, which was reduced in zVAD-fmk- (a broad spectrum caspase inhibitor) treated mice (Fig. 1E). The extent of apoptotic cell death, as evaluated by TUNEL staining, was reduced in mice treated with zVAD-fmk and in the caspase-1-dominant negative mutant transgenic mice by 50.2% and 54.0%, respectively ($n = 3$/group, $P < 0.0001$; Fig. 2A–C vs G–I, M–O and Table 1). Treatment with the caspase inhibitor was performed by placing a collagen sponge loaded with either zVAD-fmk (10 μg) or vehicle solvent and placing it over the spinal cord following the injury. TUNEL-positive cells and DNA degradation were not detected in sham-operated mice.

Caspase-1 and caspase-3 are activated following spinal cord injury

Detection of mature IL-1β has been used as a sensitive and specific marker to determine caspase-1 activation since, in mice, caspase-1 is the major (if not the only) enzyme able to cleave pro-IL-1β.[14,15,28–30] Twenty-four hours following trauma, mature IL-1β levels were 17-fold higher in vehicle-treated mice when compared with sham-operated mice ($P < 0.001$). Following SCI, zVAD-fmk treatment or mutant caspase-1 expression resulted in a 52.3% and 60.4% reduction in caspase-1 activity, respectively, when compared with traumatized wild-type untreated samples. These results demonstrate SCI-mediated caspase-1 activation, which is inhibited by local zVAD-fmk delivery or mutant caspase-1 expression (Table 2).

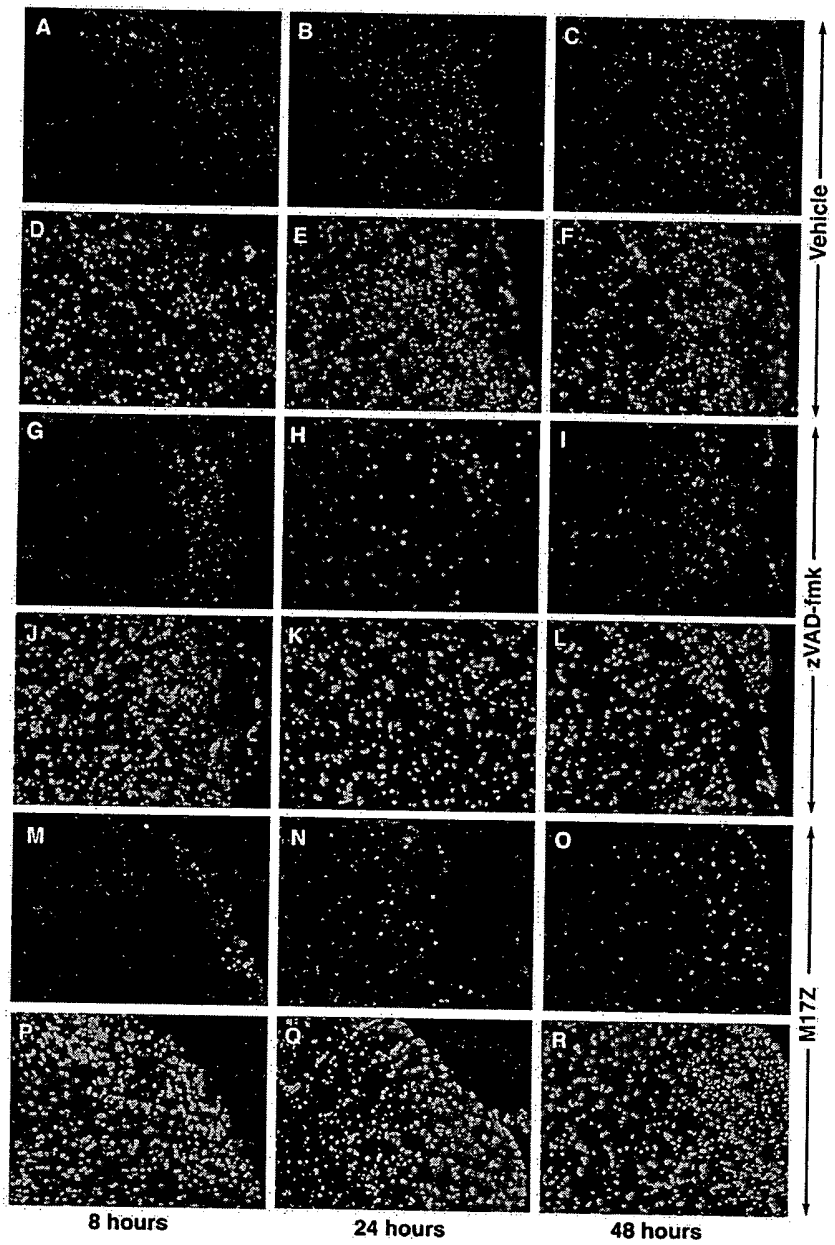

Fig. 2. Post-SCI apoptosis is inhibited by zVAD-fmk or mutant caspase-1. Under lower magnification (×5), the sections obtained from the lesion epicenter at 8 h (A, G, M), 24 h (B, H, N), and 48 h (C, I, O) following SCI show that the number of TUNEL-positive cells (green) increased over time but was reduced by zVAD-fmk treatment (G–I), or by mutant caspase-1 expression (M–O), when compared with wild-type vehicle-treated mice (A–C). (D–F, J–L, P–R) Images of the same sections as (A–C, G–I, M–O) counter-stained with Hoechst 33342.

We assayed for the active subunits of caspase-1 and caspase-3 after SCI by western blotting. The immunoreactive bands of caspase-1 (20,000 mol. wt) and caspase-3 (17,000 mol. wt) were detected in spinal cord lysates 24 h after SCI. No evidence of the active subunits was demonstrated in sham-operated mice. Detection of cleaved caspase-1 and caspase-3 immunoreactive subunits was significantly decreased in zVAD-fmk-treated mice (Fig. 3). Caspase activation can result both from autocatalysis or activation by other activated caspases.[31,32] zVAD-fmk broadly inhibits caspase activity, blocking both processing of general caspase substrates, as well as generation of activated caspase-1 and caspase-3.[33]

Table 1. Number of TUNEL-positive cells 24 h post-SCI was significantly inhibited in zVAD-fmk-treated and NSE-M17Z mice, compared with vehicle-treated wild-type mice

	Number of TUNEL-positive cells	*P*-value
Wild-type/vehicle	127.7 ± 11.1	
Wild-type/zVAD-fmk	63.6 ± 6.7	< 0.001
NSE-M17Z	58.7 ± 5	< 0.001

Cells were counted under ×40 magnification ($n = 3$/group, ANOVA).

Table 2. Mature IL-1β levels were measured using an ELISA specific for the mature form of the cytokine

	Mature IL-1β (pg/mg tissue weight)	*P*-value
Sham	0.07 ± 0.01	
SCI/vehicle	1.21 ± 0.25	< 0.001*
SCI/ZvAD-fmk	0.58 ± 0.03	= 0.01**
SCI/NSE-M17Z	0.48 ± 0.12	= 0.02***

Following spinal cord injury, mature IL-1β levels in vehicle-treated mice were 17-fold higher than in sham-operated mice. zVAD-fmk treatment and NSE-M17Z expression produced a 52.3% and 60.4% decrease, respectively, in post-SCI mature IL-1β production compared with wild-type vehicle-treated mice. Data are presented as mean ± S.E.M. and analysed by one-way ($n = 3$, ANOVA).

*P-value for comparison to sham-operated wild-type mice.

**P-value for comparison to vehicle-treated wild-type mice after spinal cord injury.

***P-value for comparison to vehicle-treated wild-type mice after spinal cord injury.

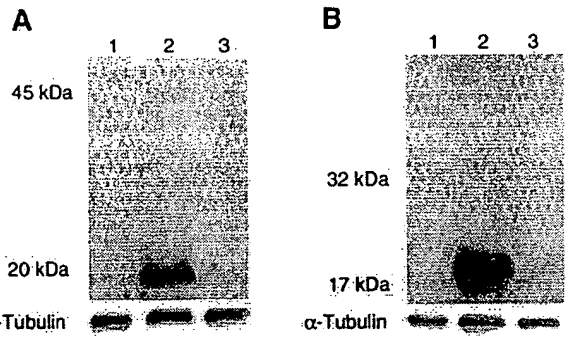

Fig. 3. Post-SCI caspase-1 and caspase-3 activation. (A) Detection of the caspase-1 active p20 subunit. (B) The caspase-3 active p17 subunit by western blot from spinal cord lysates 24 h after trauma. The active subunit was significantly reduced in zVAD-fmk-treated mice (lane 3) when compared with vehicle-treated mice (lane 2). No immunoreactive product was detected in sham-operated mouse (lane 1). These blots are representative of three independent experiments.

Detection of neuronal and non-neuronal caspase-1- and caspase-3-like signal following spinal cord injury

Significant controversy exists regarding the cell types expressing caspase-1 and caspase-3 in the central nervous system. Using the caspase-1 antibody and biotinylated DEVD-CHO (an activated caspase-3-like marker), and a specific neuronal marker to identify neurons (anti-NeuN),[34] we stained spinal cord sections from sham-operated mice. No caspase-1- or caspase-3-like staining was detected in sections from sham-operated mice (Figs 4C, 5C). However, clear caspase-1- and caspase-3-like staining was detected in both NeuN-positive and NeuN-negative cells demonstrating caspase-1- and caspase-3-like induction following SCI (Figs 4E–L, 5E–L). At the epicenter of the lesion, caspase-1- and caspase-3-like staining was detected in 77% and 69% respectively of NeuN-positive cells (345 neurons counted in three mice). As a control, preincubation with DEVD-CHO significantly blocked subsequent biotinylated DEVD-CHO binding (Fig. 5M–P). In addition, biotinylated DEVD-CHO binding colocalized with caspase-3 immunostaining (Fig. 5Q–T). No staining was detected in sections incubated with the flourescent ligand without the caspase-1 antibody or biotinylated DEVD-CHO. Cytoplasmic and nuclear caspase stainings were both detected, likely demonstrating cells in different stages of cell death. Caspase-1 contains a nuclear localization signal, and cell death-associated nuclear translocation has been previously described *in vitro*.[35] These findings are consistent with the ELISA and western blot results. In sham-operated mice, minimal mature IL-1β was detected (Table 2), and there were no detectable caspase-1 or caspase-3 immunoreactive bands (Fig. 3A, lane 1; Fig. 3B, lane 1). Furthermore, post-SCI samples demonstrated a robust increase in caspase-1 activity (Table 2) as well as marked caspase-1 p20 (Fig. 3A, lane 2) and caspase-3 p17 (Fig. 3B, lane 2) immunoreactivity. These findings show that caspase-1- and caspase-3-like signals are induced in both neuronal and non-neuronal cells following SCI.

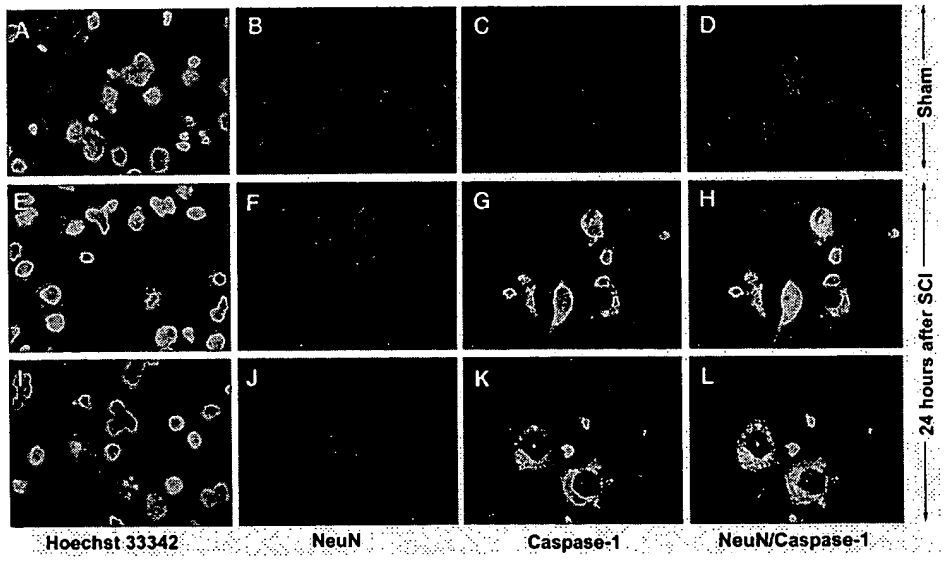

Fig. 4. Induction of neuronal and non-neuronal post-SCI caspase-1. (A–D) Spinal cord sections of a sham-operated mouse. (E–H and I–L) Two spinal cord sections at the lesion epicenter from traumatized mice 24 h following the injury. (A, E, I) Hoechst 33342 staining. (B, F, J) NeuN staining. (C, G, K) Caspase-1 staining. (D, H, L) Merged images of NeuN and caspase-1. In the merged images, both caspase-1 cytoplasmic and nuclear stainings were evident in neuronal and non-neuronal cells.

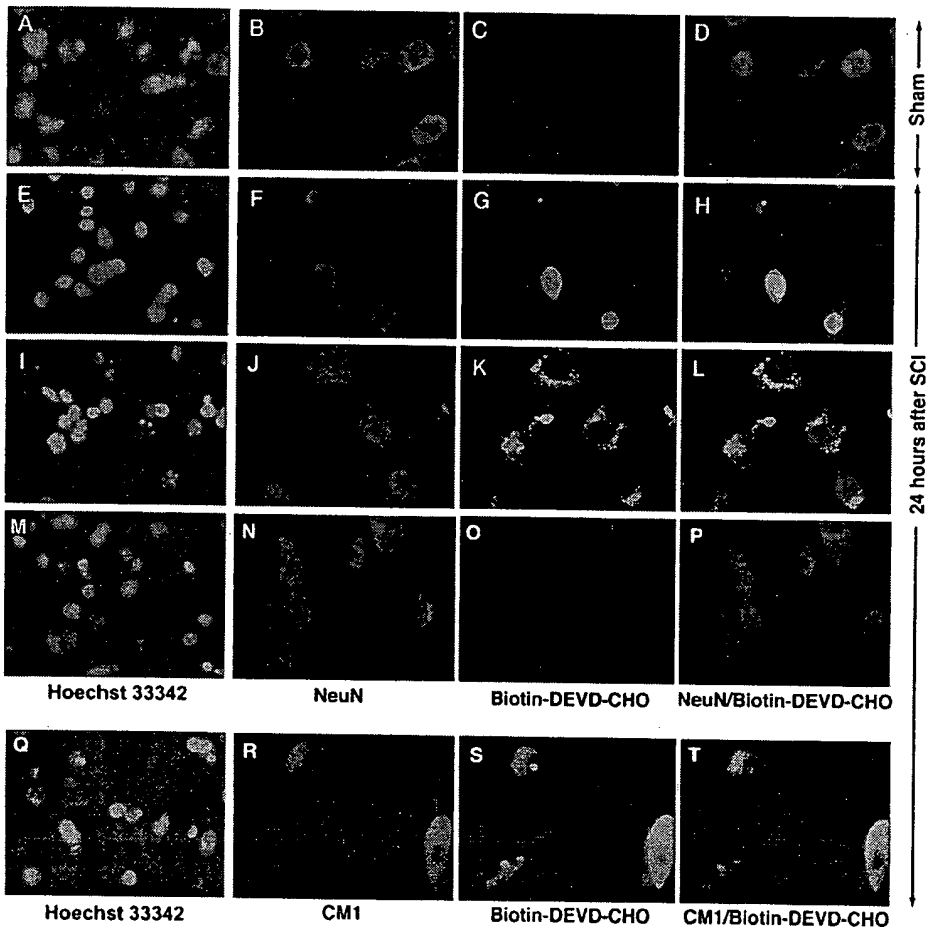

Fig. 5. Induction of neuronal and non-neuronal post-SCI caspase-3 like activity. (A–D) Spinal cord sections of a sham-operated mouse. (E–T) Spinal cord sections at the lesion epicenter from traumatized mice 24 h following the injury. (A, E, I, M, Q) Hoechst 33342 dye staining. (B, F, J, N, R) NeuN staining. (C, G, K, O, S) Active caspase-3-like staining (biotinylated DEVD-CHO). (D, H, L, P) Merged images of NeuN and caspase-3-like staining. In the merged images caspase-3-like cytoplasmic and nuclear staining were demonstrated in neuronal and non-neuronal cells. (M–P) Sections preincubated with non-biotinylated DEVD-CHO prior to biotinylated DEVD-CHO revealed blocking of specific DEVD binding (O). (Q–T) Colocalization of activated caspase-3 antibody binding (CM1) with biotinylated DEVD-CHO (T).

Post-spinal cord injury neurological deficits and lesion size are inhibited by N-*benzyloxycarbonyl-Val-Ala-Asp-fluoromethylketone and by expression of a caspase*-1-*dominant negative mutant*

To assess post-SCI neurological deficits following trauma, as well as the effect of zVAD-fmk treatment (Fig. 6A–C) and mutant caspase-1 expression (Fig. 6D–F) on motor function, a battery of tests was used by a blinded observer to evaluate the mice for a period of three weeks. All mice were paraplegic following trauma, with gradual neurological recovery over 21 days. A two-way ANOVA with repeated measures revealed significant interaction between SCI group and test time in all behavioral tests: pain withdrawal test (zVAD/control) $F_{16,79} = 42.54$, $P < 0.0001$; pain withdrawal test (M17Z/WT) $F_{13,49} = 12.78$, $P < 0.0001$; platform (zVAD/control) $F_{16,78} = 9.69$, $P < 0.0001$; platform (M17Z/WT) $F_{13,49} = 7.41$, $P < 0.0001$; open-field (zVAD/control) $F_{16,79} = 14.81$, $P < 0.0001$; open-field (M17Z/WT) $F_{13,49} = 15.39$; $P < 0.0001$.

All behavior tests, except for the platform test (zVAD-fmk/control), demonstrated a significant improvement following SCI by either zVAD-fmk treatment or mutant caspase-1 expression when compared with vehicle-treated wild-type mice. Of the zVAD-fmk-treated and caspase-1-dominant negative mice, 80% and 83%, respectively, achieved a weight bearing functional recovery (grade 3 or better on the open-field testing), compared with 13% in the control group (Fig. 6C, F). Significant differences between the two groups were not detected in any of the tests prior to day 5, suggesting that caspase inhibition does not affect the symptomatic manifestation resulting from the initial injury. However, delayed cell death, likely resulting from caspase-mediated apoptotic mechanisms, was inhibited by zVAD-fmk and by mutant caspase-1, therefore providing neurological protection from the delayed consequences of the initial injury.

To evaluate the effect of caspase inhibition, serial sections stained with Luxol Fast Blue and Cresyl Violet were examined by light microscopy for morphometric lesion analysis. The injured tissue was easily distinguished from spared tissue by a clear boundary, as demonstrated in Luxol Fast Blue-stained sections. The lesioned area was replaced by a dense astroglial scar (Fig. 7A–D). Mice treated with zVAD-fmk or expressing

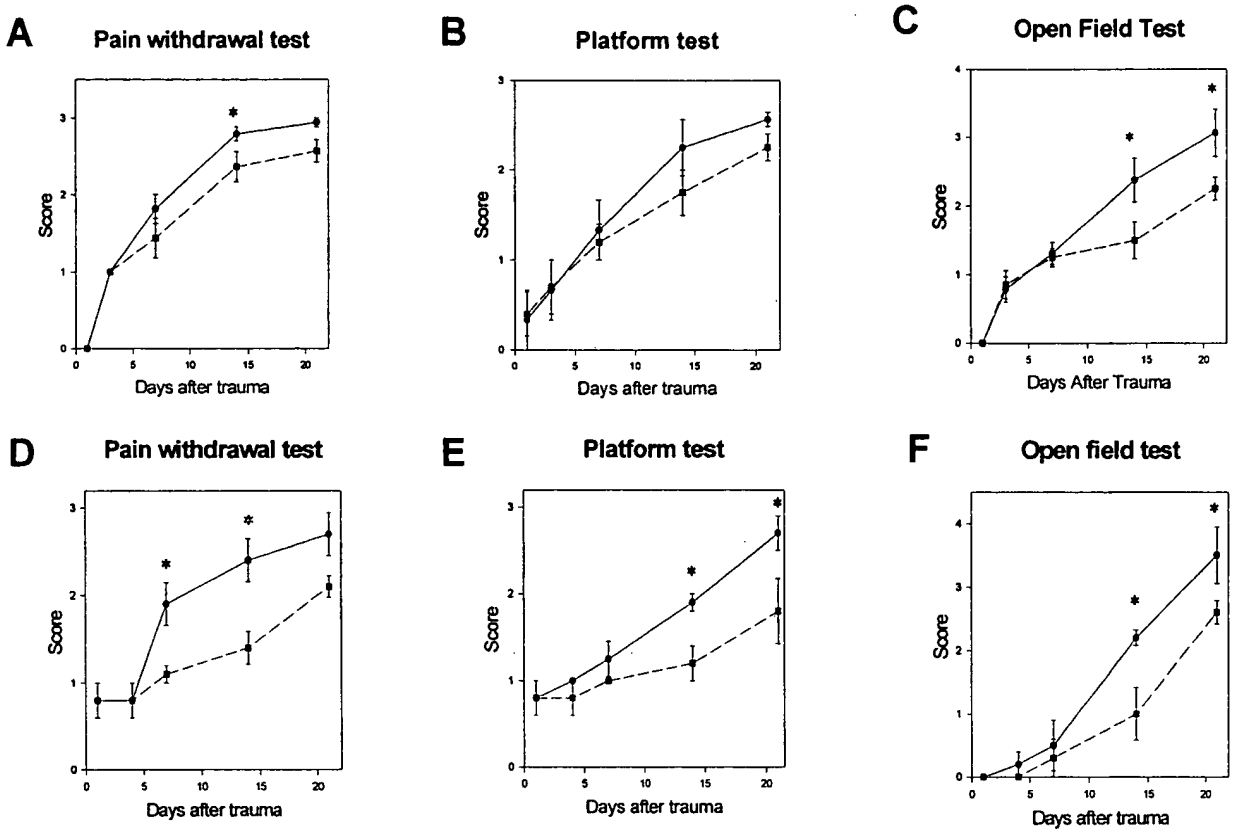

Fig. 6. zVAD-fmk and mutant caspase-1 expression improve post-SCI neurological outcome. zVAD-fmk-treated (A–C) and mutant caspase-1 transgenic (D–F) mice were blindly evaluated for a period of three weeks following trauma using the pain withdrawal test (A, D), the platform test (B, E), and the open field test (C, F). All mice were paraplegic following trauma, with gradual neurological recovery over 21 days. All three functional tests, except for the platform test (B), demonstrated a significant improvement in the zVAD-fmk-treated and mutant caspase-1 transgenic groups (circles, solid line) compared with the control (squares, dashed line) ($n = 5$–8/group, Scheffe test, $^*P < 0.05$). Significant differences were not detected prior to day five.

mutant caspase-1 had a 38.2% and 49.3% reduction in lesion size, respectively, when compared with wild-type vehicle-treated mice (Table 3, $n = 5$–8/group, ANOVA, $P < 0.05$, $P < 0.01$). In addition, to further validate our trauma model as well as the relation of the lesion size and the behavioral score, the Pearson product moment correlation was calculated between the two variables. We found a high degree of correlation between behavioral score and lesion size ($r = -0.94$, $P < 0.001$, Fig. 7E).

DISCUSSION

This study demonstrates for the first time both caspase-1 and caspase-3 activation in neuronal and non-neuronal cells following SCI. Adding therapeutic relevance to this finding, local delivery of zVAD-fmk, or use of a caspase-1-dominant negative transgenic mouse, reduced post-traumatic tissue damage and improved neurological recovery. Recently, apoptotic cell death has been detected following SCI in rats, monkeys and humans.[4,8,9] Apoptotic cell death following SCI was first detected in an experimental rat model. In a rat model, TUNEL-positive cells were detected from 4 h to three weeks after SCI, suggesting that a prolonged post-traumatic therapeutic window might exist for intervention.[4,8] Apoptotic cell death was also detected in remote degenerating fiber tracts in monkey, suggesting that apoptosis is associated with Wallerian degeneration of long spinal tracts.[4] More recently, a study of 15 patients who died between 3 h and two months after SCI reported apoptotic cell death in human spinal cords.[9] Cycloheximide, an inhibitor of protein synthesis, has been demonstrated to reduce SCI-mediated tissue damage and improve motor recovery. The beneficial effect of cycloheximide treatment might have resulted from inhibition of protein synthesis-dependent apoptosis.[8]

Since apoptotic cell death occurs in all the spinal cord cellular components, including neurons, astrocytes, oligodendrocytes, and microglia, decreased lesion size as well as improved motor function likely result from inhibition of cell death in all the different cell types.[8,36] Neuronal protection is clearly important because of the inability of neurons in the spinal cord to regenerate. Despite the fact that glia can regenerate, inhibiting glial death confers neuroprotection by at least two likely mechanisms. First, glia supply neurotrophic and metabolic support to injured neurons as well as to axonal pathways likely required for recovery of sublethal injured cells.[37–39] Second, during apoptosis, dying cells secrete additional mediators of apoptosis, such as cytokines, and free radicals, which have an additive toxic effect to other adjacent cells, likely enhancing further neurodegeneration.[40–43]

In the present study, we demonstrate that, following SCI, TUNEL-positive cells were detected in increasing numbers at 8, 24 and 48 h. TUNEL-positive cells were first detected (8 h)

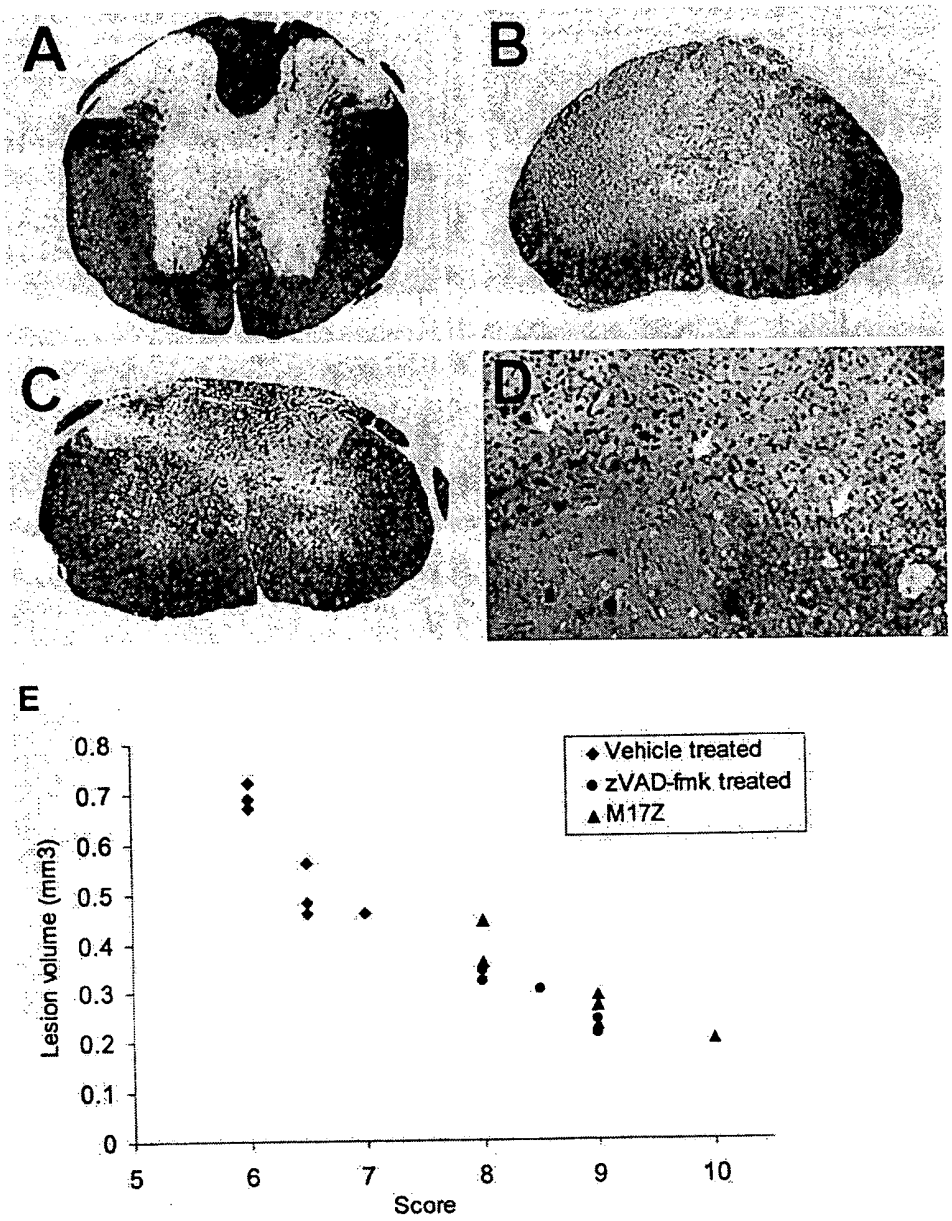

Fig. 7. zVAD-fmk and mutant caspase-1 expression reduce post-SCI tissue injury. (A–D) Spinal cord sections stained with Luxol Fast Blue and Cresyl Violet. (A) Normal spinal cord. (B, C) Representative slices at the lesion epicenter in vehicle (B) and zVAD-fmk-treated mice (C). (D) Under high magnification, there is a clear border between post-traumatic scar and normal tissue (white arrows). (E) Analysis of the correlation factor on individual mice between total behavior score (sum of the three behavioral tests at day 21) and lesion size (diamond = vehicle-treated wild type, circle = zVAD-fmk treated, and triangle = NSE-M17Z) ($r = -0.94$, $P < 0.001$, Pearson product moment correlation test).

adjacent to the site of injury where the magnitude of the triggering event is maximum. However, TUNEL-positive cells were also detected at later times (24 and 48 h) at increasing distances from the site of impact. As seen in cerebral ischemia models, this finding is consistent with a graded activation of apoptotic pathways, wherein the time for detection of TUNEL positivity is proportional to the severity of the insult.[18,44] With immunohistochemistry we demonstrated that apoptosis occurs in both neuronal and non-neuronal cells. Consistent with experimental SCI models in rats,[8] we demonstrated DNA fragmentation in the mouse weight-drop SCI model. In addition, this is the first study to demonstrate specific neuronal expression of both caspase-1 and caspase-3 following spinal cord injury.

Caspase-1 appears to play a role in tissue injury by participating in both apoptotic and inflammatory pathways. Caspase-1-mediated generation of mature IL-1β has been demonstrated to play a role in neuronal cell death as well as in inflammatory pathways.[40,42,45] Decreased tissue damage and improved neurological outcome resulting from caspase-1 inhibition likely result from interfering with both apoptotic and inflammatory pathways. Our findings do not distinguish the possible contributions to delayed neurodegeneration resulting from these two important mechanistic pathways.

Table 3. Total lesion volume four weeks after SCI in mice treated with zVAD-fmk and NSE-M17Z mice had a 38.2% and 49.3% reduction, respectively, when compared with those in vehicle-treated mice ($n = 5–8$/group, ANOVA)

	Lesion volume (mm^3)	*P*-value
Wild-type/vehicle	0.55 ± 0.04	
Wild type/zVAD-fmk	0.34 ± 0.08	< 0.05
NSE-M17Z	0.28 ± 0.03	< 0.01

Effective therapy following SCI requires a comprehensive approach targeting several potential reversible factors contributing to delayed neurological dysfunction. Local components responsible for acute post-SCI neurological deficits can be reversible or irreversible. At present, irreversible factors include cord transection and interruption of axonal pathways. If treated sufficiently early, potentially reversible factors include compression-mediated ischemia, astroglial scar formation, cell death, damage resulting from swelling, inflammation and oxidative stress.[3] Potential agents targeting different reversible factors include inhibitors of swelling and inflammation (steroids, caspase-1 inhibitors), inhibitors of scar formation (CM101), apoptosis inhibitors (caspase inhibitors), inhibitors of excitotoxins (memantine), among others.[37,46–49] As demonstrated in this study, following acute surgical decompression and stabilization, local delivery of caspase inhibitors can be one of the components of an SCI treatment protocol in humans. Unlike the case in traumatic brain injury, the localized nature of the injury makes the spinal cord particularly suited for the local delivery of a therapeutic agent such as a caspase inhibitor.

Using *in vivo* models, previous studies have demonstrated in mice that caspases are important mediators of apoptosis induced by both acute and chronic CNS insults, including brain trauma, cerebral ischemia, amyotrophic lateral sclerosis, Huntington's disease, and Parkinson's disease.[14–18] Pharmacological inhibition of caspase-1 or expression of a dominant negative caspase-1 inhibitor in transgenic mice produced substantial neurological and survival improvement in the above cell-death paradigms. Caspase-3, another important mediator of apoptosis, has also been implicated to contribute to neuronal apoptotic cell death in trauma and ischemia as well as in neurodegenerative diseases.[10,20,21,50,51] Caspase-3 activation has recently been demonstrated in human spinal cord samples following SCI.[9] Data presented here demonstrate in a mouse model that both caspase-1 and caspase-3 are activated after SCI and that pharmacological inhibition with zVAD-fmk significantly blocked their activation as well as decreased the extent of SCI-induced apoptosis. Moreover, caspase inhibition by either local delivery of zVAD-fmk or expression of a caspase-1-dominant negative mutant significantly reduced lesion size and improved motor function following SCI. These results demonstrate for the first time an important functional role for caspase-mediated apoptosis in tissue damage and neurological dysfunction following SCI. Therefore, caspase inhibition could be a rational targeted strategy for the treatment of SCI.

Acknowledgements—We thank Junying Yuan (Harvard Medical School) for providing the caspase-1 antibody and Anu Srinivasan for providing the active-caspase-3 (CM1) antibody (Idun Pharmaceuticals), Joseph R. Madsen for helpful comments, and Eugenia Friedlander for editorial assistance. This work was supported by a departmental grant and PO1 HD29587.

REFERENCES

1. Price C., Makintubee S., Herndon W. and Istre G. R. (1994) Epidemiology of traumatic spinal cord injury and acute hospitalization and rehabilitation charges for spinal cord injuries in Oklahoma. 1988–1990. *Am. J. Epidemiol.* **139,** 37–47.
2. Gerhart K. A. (1991) Spinal cord injury outcomes in a population-based sample. *J. Trauma* **31,** 1529–1535.
3. Amar A. P. and Levy M. L. (1999) Pathogenesis and pharmacological strategies for mitigating secondary damage in acute spinal cord injury. *Neurosurgery* **44,** 1027–1039.
4. Crowe M. J., Bresnahan J. C., Shuman S. L., Masters J. N. and Beattie M. S. (1997) Apoptosis and delayed degeneration after spinal cord injury in rats and monkeys. *Nat. Med.* **3,** 73–76.
5. Lou J., Lenke L. G., Ludwig F. J. and O'Brien M. F. (1998) Apoptosis as a mechanism of neuronal cell death following acute experimental spinal cord injury. *Spinal Cord* **36,** 683–690.
6. Braughler J. M. and Hall E. D. (1985) Current application of "high-dose" steroid therapy for CNS injury. A pharmacological perspective. *J. Neurosurg.* **62,** 806–810.
7. Yong C., Arnold P. M., Zoubine M. N., Citron B. A., Watanabe I., Berman N. E. and Festoff B. W. (1998) Apoptosis in cellular compartments of rat spinal cord after severe contusion injury. *J. Neurotrauma* **15,** 459–472.
8. Liu X. Z., Xu X. M., Hu R., Du C., Zhang S. X., McDonald J. W., Dong H. X., Wu Y. J., Fan G. S., Jacquin M. F., Hsu C. Y. and Choi D. W. (1997) Neuronal and glial apoptosis after traumatic spinal cord injury. *J. Neurosci.* **17,** 5395–5406.
9. Emery E., Aldana P., Bunge M. B., Puckett W., Srinivasan A., Keane R. W., Bethea J. and Levi A. D. (1998) Apoptosis after traumatic human spinal cord injury. *J. Neurosurg.* **89,** 911–920.
10. Springer J. E., Azbill R. D. and Knapp P. E. (1999) Activation of the caspase-3 apoptotic cascade in traumatic spinal cord injury. *Nat. Med.* **5,** 943–946.
11. Miura M., Zhu H., Rotello R., Hartwieg E. A. and Yuan J. (1993) Induction of apoptosis in fibroblasts by IL-1 beta-converting enzyme, a mammalian homolog of the *C. elegans* cell death gene ced-3. *Cell* **75,** 653–660.
12. Friedlander R. M. and Yuan J. (1998) ICE, neuronal apoptosis and neurodegeneration. *Cell Death Differ.* **5,** 823–831.
13. Friedlander R. M., Brown R. H., Gagliardini V., Wang J. and Yuan J. (1997) Inhibition of ICE slows ALS in mice. *Nature* **388,** 31.
14. Friedlander R. M., Gagliardini V., Hara H., Fink K. B., Li W., MacDonald G., Fishman M. C., Greenberg A. H., Moskowitz M. A. and Yuan J. (1997) Expression of a dominant negative mutant of interleukin-1 beta converting enzyme in transgenic mice prevents neuronal cell death induced by trophic factor withdrawal and ischemic brain injury. *J. exp. Med.* **185,** 933–940.
15. Hara H., Friedlander R. M., Gagliardini V., Ayata C., Fink K., Huang Z., Shimizu-Sasamata M., Yuan J. and Moskowitz M. A. (1997) Inhibition of interleukin-1beta converting enzyme family proteases reduces ischemic and excitotoxic neuronal damage. *Proc. natn. Acad. Sci. USA* **94,** 2007–2012.
16. Ona V. O., Li M., Vonsattel J. P., Andrews L. J., Khan S. Q., Chung W. M., Frey A. S., Menon A. S., Li X. J., Stieg P. E., Yuan J., Penney J. B., Young A. B., Cha J. H. and Friedlander R. M. (1999) Inhibition of caspase-1 slows disease progression in a mouse model of Huntington's disease. *Nature* **399,** 263–267.
17. Klevenyi P., Andreassen O., Ferrante R. J., Schleicher J. R. Jr., Friedlander R. M. and Beal M. F. (1999) Transgenic mice expressing a dominant negative mutant interleukin-1beta converting enzyme show resistance to MPTP neurotoxicity. *NeuroReport* **10,** 635–638.

18. Hara H., Fink K., Endres M., Friedlander R. M., Gagliardini V., Yuan J. and Moskowitz M. A. (1997) Attenuation of transient focal cerebral ischemic injury in transgenic mice expressing a mutant ICE inhibitory protein. *J. cerebr. Blood Flow Metab.* **17,** 370–375.
19. Fink K. B., Andrews L. J., Butler W. E., Ona V. O., Li M., Bogdanov M., Endres M., Khan S. Q., Namura S., Stieg P. E., Beal M. F., Moskowitz M. A., Yuan J. and Friedlander R. M. (1999) Reduction of post-traumatic brain injury and free radical production by inhibition of the caspase-1 cascade. *Neuroscience* **94,** 1213–1218.
20. Yakovlev A. G., Knoblach S. M., Fan L., Fox G. B., Goodnight R. and Faden A. I. (1997) Activation of CPP32-like caspases contributes to neuronal apoptosis and neurological dysfunction after traumatic brain injury. *J. Neurosci.* **17,** 7415–7424.
21. Namura S., Zhu J., Fink K., Endres M., Srinivasan A., Tomaselli K. J., Yuan J. and Moskowitz M. A. (1998) Activation and cleavage of caspase-3 in apoptosis induced by experimental cerebral ischemia. *J. Neurosci.* **18,** 3659–3668.
22. Burne J. F., Staple J. K. and Raff M. C. (1996) Glial cells are increased proportionally in transgenic optic nerves with increased numbers of axons. *J. Neurosci.* **16,** 2064–2073.
23. Forss-Petter S., Danielson P. E., Catsicas S., Battenberg E., Price J., Nerenberg M. and Sutcliffe J. G. (1990) Transgenic mice expressing beta-galactosidase in mature neurons under neuron-specific enolase promoter control. *Neuron* **5,** 187–197.
24. Kuhn P. L. and Wrathall J. R.. (1998) A mouse model of graded contusive spinal cord injury. *J. Neurotrauma* **15,** 125–140.
25. Sambrook J., Fritch E. F. and Maniatis T. (1989) Analysis and cloning of eukaryotic genomic DNA. In *Molecular Clonning* (eds Ford N., Nolan C. and Ferguson M.), pp. 9.16–9.19. Cold Spring Harbour Laboratory Press, New York.
26. Mattson M. P., Keller J. N. and Begley J. G. (1998) Evidence for synaptic apoptosis. *Expl Neurol.* **153,** 35–48.
27. Xu D., Bureau Y., McIntyre D. C., Nicholson D. W., Liston P., Zhu Y., Fong W. G., Crocker S. J., Korneluk R. G. and Robertson G. S. (1999) Attenuation of ischemia-induced cellular and behavioral deficits by X chromosome-linked inhibitor of apoptosis protein overexpression in the rat hippocampus. *J. Neurosci.* **19,** 5026–5033.
28. Li P., Allen H., Banerjee S., Franklin S., Herzog L., Johnston C., McDowell J., Paskind M., Rodman L. and Salfeld J. (1995) Mice deficient in IL-1 beta-converting enzyme are defective in production of mature IL-1 beta and resistant to endotoxic shock. *Cell* **80,** 401–411.
29. Kuida K., Lippke J. A., Ku G., Harding M. W., Livingston D. J., Su M. S. and Flavell R. A. (1995) Altered cytokine export and apoptosis in mice deficient in interleukin-1 beta converting enzyme. *Science* **267,** 2000–2003.
30. Miura M., Friedlander R. M. and Yuan J. (1995) Tumor necrosis factor-induced apoptosis is mediated by a CrmA-sensitive cell death pathway. *Proc. natn. Acad. Sci. USA* **92,** 8318–8322.
31. Thornberry N. A., Bull H. G., Calaycay J. R., Chapman K. T., Howard A. D., Kostura M. J., Miller D. K., Molineaux S. M., Weidner J. R. and Aunins J. (1992) A novel heterodimeric cysteine protease is required for interleukin-1 beta processing in monocytes. *Nature* **356,** 768–774.
32. Nicholson D. W. (1999) Caspase structure, proteolytic substrates, and function during apoptotic cell death. *Cell Death Differ.* **6,** 1028–1042.
33. Garcia-Calvo M., Peterson E. P., Leiting B., Ruel R., Nicholson D. W. and Thornberry N. A. (1998) Inhibition of human caspases by peptide-based and macromolecular inhibitors. *J. biol. Chem.* **273,** 32608–32613.
34. Mullen R. J., Buck C. R. and Smith A. M. (1992) NeuN, a neuronal specific nuclear protein in vertebrates. *Development* **116,** 201–211.
35. Mao P. L., Jiang Y., Wee B. Y. and Porter A. G. (1998) Activation of caspase-1 in the nucleus requires nuclear translocation of pro-caspase-1 mediated by its prodomain. *J. biol. Chem.* **273,** 23621–23624.
36. Shuman S. L., Bresnahan J. C. and Beattie M. S. (1997) Apoptosis of microglia and oligodendrocytes after spinal cord contusion in rats. *J. Neurosci. Res.* **50,** 798–808.
37. Lee T. T., Green B. A., Dietrich W. D. and Yezierski R. P. (1999) Neuroprotective effects of basic fibroblast growth factor following spinal cord contusion injury in the rat. *J. Neurotrauma* **16,** 347–356.
38. McTigue D. M., Horner P. J., Stokes B. T. and Gage F. H. (1998) Neurotrophin-3 and brain-derived neurotrophic factor induce oligodendrocyte proliferation and myelination of regenerating axons in the contused adult rat spinal cord. *J. Neurosci.* **18,** 5354–5365.
39. Abe Y., Yamamoto T., Sugiyama Y., Watanabe T., Saito N., Kayama H. and Kumagai T. (1999) Apoptotic cells associated with Wallerian degeneration after experimental spinal cord injury: a possible mechanism of oligodendroglial death. *J. Neurotrauma* **16,** 945–952.
40. Friedlander R. M., Gagliardini V., Rotello R. J. and Yuan J. (1996) Functional role of interleukin 1 beta (IL-1 beta) in IL-1 beta-converting enzyme-mediated apoptosis. *J. exp. Med.* **184,** 717–724.
41. Prehn J. H., Jordan J., Ghadge G. D., Preis E., Galindo M. F., Roos R. P., Krieglstein J. and Miller R. J. (1997) Ca^{2+} and reactive oxygen species in staurosporine-induced neuronal apoptosis. *J. Neurochem.* **68,** 1679–1685.
42. Troy C. M., Stefanis L., Prochiantz A., Greene L. A. and Shelanski M. L. (1996) The contrasting roles of ICE family proteases and interleukin-1beta in apoptosis induced by trophic factor withdrawal and by copper/zinc superoxide dismutase down-regulation. *Proc. natn. Acad. Sci. USA* **93,** 5635–5640.
43. Diaz-Ruiz A., Rios C., Duarte I., Correa D., Guizar-Sahagun G., Grijalva I. and Ibarra A. (1999) Cyclosporin-A inhibits lipid peroxidation after spinal cord injury in rats. *Neurosci. Lett.* **266,** 61–64.
44. Endres M., Namura S., Shimizu-Sasamata M., Waeber C., Zhang L., Gomez-Isla T., Hyman B. T. and Moskowitz M. A. (1998) Attenuation of delayed neuronal death after mild focal ischemia in mice by inhibition of the caspase family. *J. cerebr. Blood Flow Metab.* **18,** 238–247.
45. Dinarello C. A. (1998) Interleukin-1 beta, interleukin-18, and the interleukin-1 beta converting enzyme. *Ann. N. Y. Acad. Sci.* **856,** 1–11.
46. Bracken M. B., Shepard M. J., Holford T. R., Leo-Summers L., Aldrich E. F., Fazl M., Fehlings M., Herr D. L., Hitchon P. W., Marshall L. F., Nockels R. P., Pascale V., Perot P. L. Jr., Piepmeier J., Sonntag V. K., Wagner F., Wilberger J. E., Winn H. R. and Young W. (1997) Administration of methylprednisolone for 24 or 48 hours or tirilazad mesylate for 48 hours in the treatment of acute spinal cord injury. Results of the Third National Acute Spinal Cord Injury Randomized Controlled Trial. National Acute Spinal Cord Injury Study. *J. Am. med. Ass.* **277,** 1597–1604.
47. Wamil A. W., Wamil B. D. and Hellerqvist C. G. (1998) CM101-mediated recovery of walking ability in adult mice paralyzed by spinal cord injury. *Proc. natn. Acad. Sci. USA* **95,** 13188–13193.
48. Chen H. S. and Lipton S. A. (1997) Mechanism of memantine block of NMDA-activated channels in rat retinal ganglion cells: uncompetitive antagonism. *J. Physiol., Lond.* **499,** 27–46.
49. Chen H. S., Pellegrini J. W., Aggarwal S. K., Lei S. Z., Warach S., Jensen F. E. and Lipton S. A. (1992) Open-channel block of *N*-methyl-D-aspartate (NMDA) responses by memantine: therapeutic advantage against NMDA receptor-mediated neurotoxicity. *J. Neurosci.* **12,** 4427–4436.
50. Goldberg Y. P., Nicholson D. W., Rasper D. M., Kalchman M. A., Koide H. B., Graham R. K., Bromm M., Kazemi-Esfarjani P., Thornberry N. A., Vaillancourt J. P. and Hayden M. R. (1996) Cleavage of huntingtin by apopain, a proapoptotic cysteine protease, is modulated by the polyglutamine tract. *Nat. Genet.* **13,** 442–449.
51. Gervais F. G., Xu D., Robertson G. S., Vaillancourt J. P., Zhu Y., Huang J., LeBlanc A., Smith D., Rigby M., Shearman M. S., Clarke E. E., Zheng H., Van Der Ploeg L. H., Ruffolo S. C., Thornberry N. A., Xanthoudakis S., Zamboni R. J., Roy S. and Nicholson D. W. (1999) Involvement of caspases in proteolytic cleavage of Alzheimer's amyloid-beta precursor protein and amyloidogenic A beta peptide formation. *Cell* **97,** 395–406.

(*Accepted* 7 *April* 2000)